

THE EFFECT OF WIND STRESS ON WAVE OVERTOPPING ON VERTICAL SEAWALL

Sara Tuozzo¹, Angela Di Leo², Mariano Buccino¹, Fabio Dentale², Eugenio Pugliese Carratelli²
and Mario Calabrese¹

Onshore wind can significantly affect wave overtopping process and increase mean overtopping discharge. Thus, the wind should be an important variable in coastal design process. However, despite many researches have analyzed the influence of wind on the overtopping, there is still a lack of exhaustive knowledge about this phenomenon. To further analyze the wind effects, the CFD model FLOW-3D has been used to investigate wave overtopping at vertical seawalls. The single-fluid approach has been adopted, i.e. the presence of wind has been simulated via the wind shear stress on the sea surface. The main aim of this work is to verify the ability of this simplified numerical modelling to capture the macro-processes involved in the phenomenon of wave overtopping. The presence of wind shear stress has led to physically consistent results. It confirmed that as the mean overtopping discharge decreases, as the wind effect increases. Furthermore, numerical results have shown that the advection of water droplets behind the structure by the wind is the key mechanism for the enhancement of wave overtopping. Finally, by gathering numerical results and laboratory data carried out by Durbridge (2021), a new predictive formula to estimate the wind factor is provided.

Keywords: wind modelling; wind shear stress; wind factor; Computational Fluid Dynamics

INTRODUCTION

The onshore wind that blows during storms can significantly enhance wave run-up and overtopping, increasing the risk of coastal flooding and jeopardizing people safety. As indicated in the EurOtop 2018 manual, the influence of wind on green water overtopping is negligible, while it might increase by up four times discharges of the order of 1 l/s/m, which represents the threshold for structural damages and pedestrians and vehicles safety. Therefore, wind should be an important variable to account for in the design of coastal defenses against flooding.

However, despite researchers have been studying the influence of wind on wave overtopping since the end of the last century, the full understanding and correct assessment of its effects is still fraught with uncertainty. Most of the literature, indeed, has investigated this phenomenon through physical modelling (among the others, de Waal 1996, Wolters 2007, Durbridge 2021), experiencing some difficulties as both Froude and Reynolds scales are needed to analyze the wind effect on the overtopping process. On the other hand, a few numerical studies have examined this phenomenon (Kiku and Kawasaki 2014, Hieu 2014, Xie 2014., Di Leo et al., 2022), although numerical models have the advantage of avoiding scale effects associated with laboratory experiments. Moreover, only a few studies have proposed predictive equation to quantitatively estimate the influence of wind on wave overtopping. The formula provided by Pullen et al. (2009), obtained by gathering field and laboratory data, relates the wind transport factor f_{WIND} (i.e. the ratio of mean overtopping discharge with and without wind) to the overtopping regime, and argues that the wind only affects discharge lower than 10 l/s/m approximately. Nonetheless, they neglect the possible influence of other variables on the wind factor, such as the wind speed. More recently, Murakami et al. (2020) proposed a new equation based on laboratory experiments in which the wind factor is a function of wind speed, wave characteristics and the crest freeboard of the structure. However, it might underestimate the effect of wind since only the water flow on the seawall crown was taken into account (the advection of splash beside the structure due to the wind was neglected).

In this study, we use a CFD numerical model to assess the role of wind on the mean overtopping discharge at a vertical seawall. In particular, the CFD multi-physics solver FLOW-3D HYDRO (Flow Science 2022) has been employed, which can reproduce the presence of wind using either a single or a two-fluids approach. Among them, we have adopted the former technique that models the wind by the shear stress it exerts on the sea surface. Despite the less rigorous modelling, we aim to demonstrate that it is sufficient to reproduce the macro-feature of the phenomenon, namely the growth of the overtopping rate due to the wind.

Specifically, we have tried to clarify what is the key mechanism by which the wind causes the enhancement of the overtopping rate and to figure out the variables that must be taken into account in order to quantify this enhancement. Finally, we have developed a new predictive equation for the wind factor.

¹ Department of Civil, Architectural and Environmental Engineering, University of Napoli Federico II, Via Claudio 21, Napoli, 80125, Italy

² Department of Civil Engineering, University of Salerno, Via Giovanni Paolo II 132, Fisciano, 84084, Italy

EXPERIMENTS

Numerical model

In the current study, the CFD code FLOW-3D HYDRO has been used due to its reliability to deal with wave-structure interaction problems, as demonstrated in previous works (Dentale et al. 2018, Buccino et al. 2019a, b).

FLOW-3D HYDRO solves the Reynolds-Averaged Navier–Stokes (RANS) equations using an Eulerian approach under the assumption of incompressible fluid flow. Imposing continuity within the flow, the following system is then solved:

$$\frac{\partial u_i}{\partial x_i} = 0 \quad (1)$$

$$\frac{\partial u_i}{\partial t} + u_j \frac{\partial u_i}{\partial x_j} + \frac{1}{\rho} \frac{\partial p}{\partial x_i} - \frac{\partial}{\partial x_j} \left[(v + \nu_T) \left(\frac{\partial u_i}{\partial x_j} + \frac{\partial u_j}{\partial x_i} \right) \right] - g_i = 0 \quad (2)$$

where u is the time averaged velocity, ρ is the fluid density, p is the pressure, ν is the kinematic viscosity, ν_T is the eddy viscosity and g is the gravity acceleration. The eddy viscosity ν_T is determined through the RNG k- ε model (Yakot and Smith 1992), with the equations for the turbulent kinetic energy k and the specific turbulent dissipation ε , as follows:

$$\frac{\partial k}{\partial t} + u_j \frac{\partial k}{\partial x_j} - \frac{\partial}{\partial x_j} \left[\frac{(v + \nu_T)}{\sigma_k} \frac{\partial k}{\partial x_j} \right] + \varepsilon - P = 0 \quad (3)$$

$$\frac{\partial \varepsilon}{\partial t} + u_j \frac{\partial \varepsilon}{\partial x_j} - \frac{\partial}{\partial x_j} \left[\frac{(v + \nu_T)}{\sigma_\varepsilon} \frac{\partial \varepsilon}{\partial x_j} \right] + c_2 \frac{\varepsilon^2}{k} - c_1 \frac{\varepsilon}{k} \nu_T P + R = 0 \quad (4)$$

The Eqs. 1-4 are integrated on a mesh of fixed rectangular cells with a finite-difference scheme, a staggered grid arrangement is adopted. The free surface is tracked according to the Volume of Fluid (VOF) technique (Hirt and Nichols 1981). In this volume-of-fluid (VOF) approach, the fraction F of the cell filled with fluid is stored: $F = 0$ outside the fluid domain (void region), $F = 1$ within the interior of the fluid, and $0 < F < 1$ for cells that contained the free surface. Curved obstacles, wall boundaries, or other geometric features are embedded in the mesh by defining the fractional areas of the cells that are open to flow (FAVOR™ method) (Hirt and Sicilian 1985).

To maintain the stability and accuracy of the solution, a variable time-stepping is implemented. In particular, the n^{th} time step is automatically selected as the minimum between the user-specified time step and a convergence time step, Δt^{CON} , needed to avoid numerical instabilities. Since the advective fluxes have been computed using a simple first order donor cell, Δt^{CON} is required to meet the following criterion:

$$\Delta t^{\text{CON}} = \min(0.5 \cdot \Delta t_{\text{CFL}}, 0.5 \frac{\Delta x}{\sqrt{\Delta z \Delta a_z}}) \quad (5)$$

where Δt_{CFL} is the time step to satisfy the Courant–Friedrichs–Lewy (CFL) stability criterion, and the second quantity at the right-hand side of Eq. 5 ensures surface waves cannot propagate more than one cell at time step (a_z indicates vertical acceleration).

As mentioned in the previous section, the wind has been modelled introducing in the RANS equations the shear stress that it exerts on the sea surface. If the vertical distribution of the sea wind follows logarithmic law, the wind shear stress acting on the sea surface is typically estimated by:

$$\vec{\tau}_s = \rho_a C_{D10} |\vec{U}_{10}| U_{10} \quad (6)$$

where ρ_a is the density of air (1.225 kg/m³), U_{10} is the wind velocity at 10 m above the sea surface and C_{D10} is the wind shear coefficient (or drag coefficient).

Experimental setup

Numerical experiments aim to analyze the enhancement of wave overtopping at a vertical seawall due to the wind. The numerical experiments were performed at prototype scale.

According to the literature, as the overtopping discharge diminishes, as the influence of wind increases. Therefore, crest freeboard of vertical seawall, R_c , has been varied in order to obtain different order of magnitude of overtopping discharge ($10^{-1} \div 10^2$ l/s/m). Fig.1a shows seven different values of R_c simulated, which varies from 2.23 to 9.27 m. The vertical seawall is located at the end of a multi-slope foreshore (Fig.1b), which represents a schematization of the Havana foreshore investigated during an experimental campaign conducted at the University of Napoli Federico II (Lopez et al. 2015, 2016).

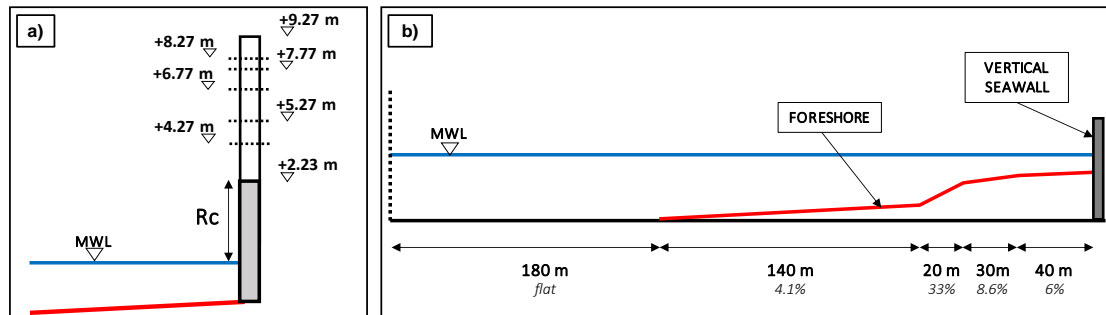


Figure 1. Characteristics of the foreshore and vertical seawalls reproduced in the numerical model. Panel a) seven different crest freeboards investigated; panel b) the bathymetry and the vertical seawall reproduced in the numerical flume.

Both breaking and non-breaking waves have been investigated; the wave height varies from 1.5m to 8m and two wave periods have been examined (10s and 12s).

The wind speeds simulated, U_{10} , derive from the sea age parameter β , i.e. deep water wave celerity to wind speed ratio, which characterizes wave condition under the action of wind (Bretschneider 1964), Table 1. Specifically, values of β ranging from 0.5 to 1.25 represent seas under the dominant effect of tangential wind stress; larger values, up to 10, characterize swells under weak winds.

Crest freeboards investigated for each wave condition, as well as the wind conditions, are reported in Table 2. 34 experiments have been performed.

$C_0 = 15.61$ m/s		$C_0 = 18.74$ m/s	
β [-]	U_{10} [m/s]	β [-]	U_{10} [m/s]
0.50	31.2	0.62	30.0
0.82	19.0	1.00	18.7
1.25	12.5	2.00	9.4
3.00	5.2	3.07	6.1
5.04	3.1	9.86	1.9

	H [m]	T [s]	C_0 [m/s]	R_c [m]	U_{10} [m/s]
TEST_1	8.0	10.0	15.61	8.27; 9.27	3.1 ÷ 31.2
TEST_2	8.0	12.0	18.74	2.23	1.9 ÷ 30.0
TEST_3	5.4	10.0	15.61	2.23; 9.27	3.1 ÷ 31.2
TEST_4	1.5	10.0	15.61	2.23 ÷ 9.27	3.1 ÷ 31.2

The drag coefficient required in Eq. 6 has been estimated using the formula of Andreas et al. (2012), which is one of the most recent and accurate formulations for wind drag:

$$\sqrt{C_{D10}} = \frac{0.239 + 0.0433 \cdot \{(U_{10} - 8.271) + [0.120 \cdot (U_{10} - 8.271)^2 + 0.181]^{0.5}\}}{U_{10}} \quad (7)$$

CFD numerical setup

A 2D-numerical wave flume was set up to carry out the numerical simulations. The bathymetry and the structure characteristics described in the previous section are generated using a CAD software, and then imported into the code as an STL file.

The computational domain had only a general mesh block; a rectangular cell has been adopted (0.4x0.4x0.15m). Previously, a grid sensitivity study based on the final overtopping volume was performed, which is described in (Di Leo et al. 2022a,b) and omitted here for sake of brevity.

Numerical waves were generated at the boundary condition by using the Stokes and Cnoidal (Fourier series method, Fenton (1999)) wave generator. The waves enter the computational domain and propagates in the direction normal to the boundary. At the opposite side, behind the vertical seawall, an “Outflow” condition has imposed, which lets the waves flow out the computational domain without any reflections. The lateral boundaries are characterized by a “Symmetry” condition, where the velocity gradient vanishes, and the turbulence production is zero. At the bottom, the “Wall” condition has defined, which applies a zero-velocity condition normal to the boundary.

Finally, a list of relevant numerical parameter settings of the present study is given in Table 3.

Parameter	Settings
Fluid	Water (20°); incompressible
Turbulence	RNG
Pressure solver	GMRES
VOF advection	Split Lagrangian method (TruVof)
Time step control	Automatic (stability and convergence)

RESULTS

Physical processes

As observed by the literature (e.g. de Waal 1996 and Resio 1987), the wind can affect wave overtopping either by raising the mean sea level ($\bar{\eta}$) or by acting on the wave profile at the wall. The primary aim is to assess whether the simply wind modelling adopted in this study (i.e. single fluid technique) is able to reproduce such behaviors.

The effect on mean sea level includes either a direct effect, wind setup, or an indirect effect, wave setup. The effect on wave profile encompasses the change in phase-averaged and time-domain wave properties (e.g., variation of the wave height and breaking point), the deformation of the run-up wedge, or the advection behind the structure of the droplets produced during the up-rush process.

As concerns the wind setup, it is ruled by the cross-shore balance between the time-averaged wind stress and the hydrostatic forces, which can be integrated and parametrized in terms of the quantity A (i.e. the shear to hydrostatic force ratio):

$$A = (n \cdot \bar{\tau}_w \cdot l_D) / \rho_w g h_0^2 \quad (8)$$

where n accounts for the effects of bottom friction, l_D is the domain’s length and h_0 is the offshore water depth. However, even if the maximum wind speed investigated is considered ($U_{10} = 31.2$ m/s), the parameter A equals 4.7×10^{-4} , indicating that the role of shear forces can be assumed to be negligible. The length of the computational domain is too small (410m) to allow a significant wind setup.

The indirect effect on wave setup is due to the variation in breaking point generated by the presence of wind. An increase in wave energy caused by the wind leads to an increase in the radiation stress gradient, that produces a greater setup or set-down for breaking and non-breaking wave respectively. As can be observed in Fig.2, the wind shear stress reproduces the aforementioned correlation. This is except for two outliers circled in the figure, for which mean sea level reduces due to a reforming/rebreaking process that occurs in the innermost part of the foreshore.

Overall, Fig.2 demonstrates that for the numerical domain investigated, the variations in mean sea water level due to wind are too small (lower than 5%) to have a significant effect on the mean overtopping discharge.

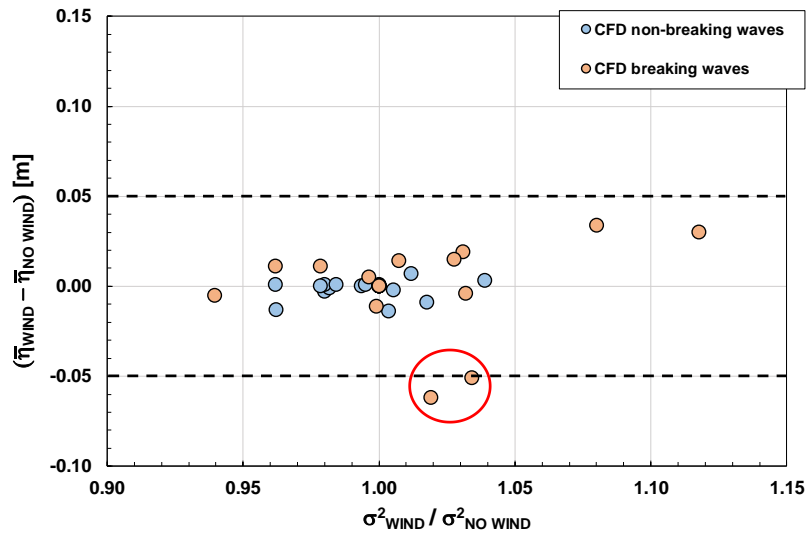


Figure 2. Variation of mean sea level due to the presence of wind as a function of the profile variance ratio, namely the variation of wave energy due to the wind.

Analyzing the influence of the wind on wave profile, the effects may be different for breaking and non-breaking wave.

As suggested by Kiku and Kawasaki (2014), the presence of wind enhances run-up wedge and pushes forward the droplets that otherwise would fall back into the sea. Figs. 3a,b show that CFD model well reproduces both the mechanisms, which lead to a consequent increase in the overtopping rate (Fig. 3c).

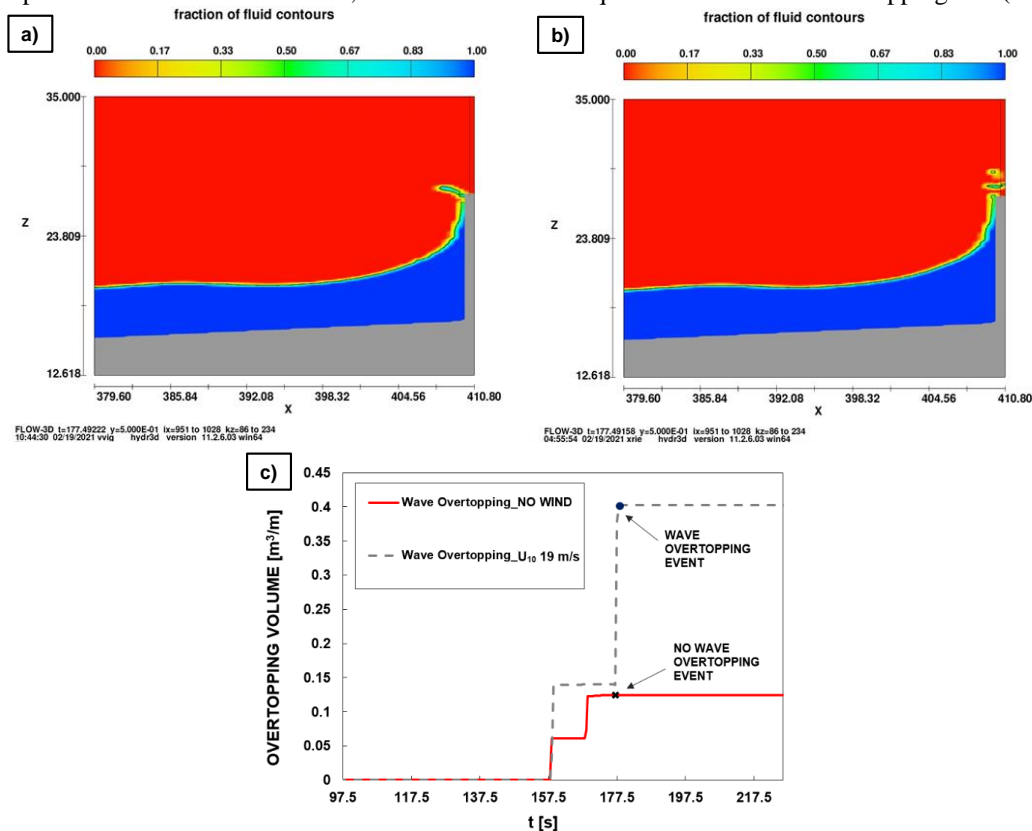


Figure 3. Effects of the wind either on the run-up wedge or on the advection of the droplets behind the seawall. TEST_3 and R_c 6.77m at the time 177.5s. Panel a) no wind condition; panel b) wind U_{10} 19.0 m/s; panel c) comparison between cumulative overtopping volume curves with and without wind.

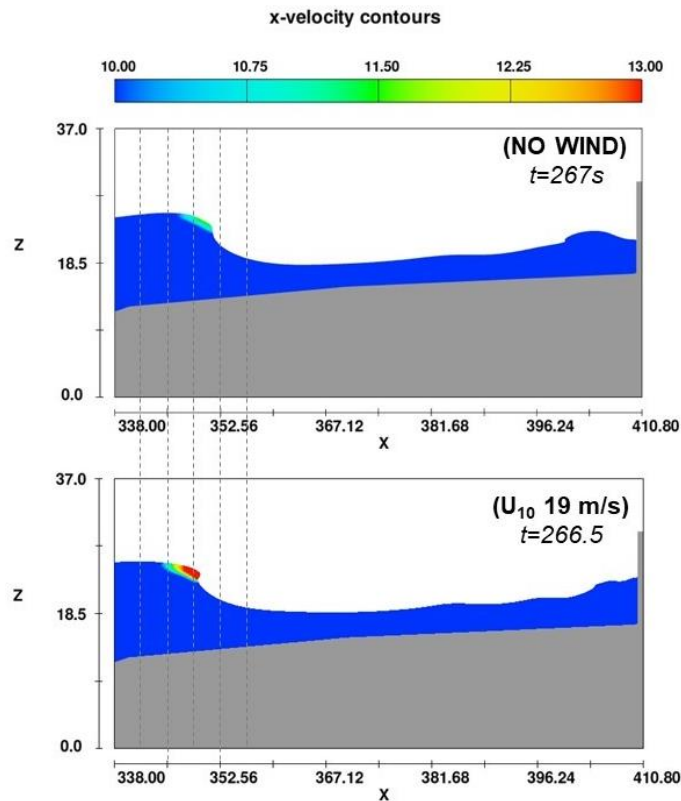


Figure 4. Variation in the breaking point due to the presence of wind, TEST_1 and R_c 8.27m.

On the other hand, for breaking waves the wind may reduce the overtopping rate. The presence of wind moves seaward the breaking point (Fig.4), as observed by Perlin et al. (2013). As greater the surf zone, as greater the energy dissipation, which eventually results in a lower amount of wave overtopping. However, this is not a systematic behavior. A reduction in wave overtopping has not been observed for all breaking waves investigated. Indeed, as the order of magnitude of discharge reduces, as the wind enhances the overtopping rate both for breaking and non-breaking waves.

Finally, we have verified the ability of wind modelling adopted to properly reproduce the enhancement of the overtopping rate due to the wind. To this end, a qualitative comparison has been performed between the CFD outcomes and the physical results carried out by the laboratory experiments of Pullen et al. (2009), which have tested the same range of wind speed (Fig. 5).

The comparison shows that the influence of the wind shear stress on the overtopping is consistent with those observed during the experiments. Laboratory data demonstrate that the wind effect increases as the overtopping discharge decreases. Numerical outcomes well reproduce this behavior; although more scattered, CFD data spread within the same cloud of Pullen et al.' results. Furthermore, as reported in de Waal et al. 1996 and in Pullen et al. 2009, the wind shear stress confirms that the influence of wind is negligible for green wave overtopping (i.e. $q_{NO-WIND}$ larger than $O(10^2)$ l/s/m).

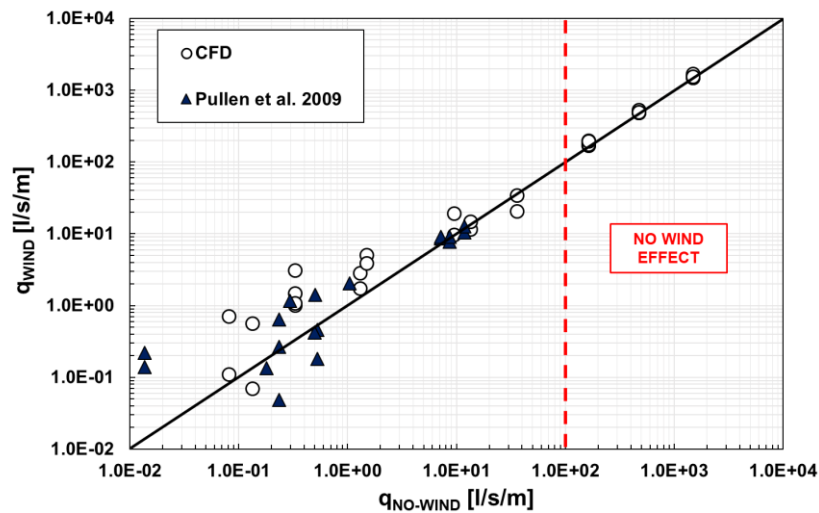


Figure 5. Comparison between CFD and physical results obtained by Pullen et al. (2009).

A further qualitative analysis has been carried out to understand the variation in the wind effects depending on the magnitude of overtopping discharge. Fig. 6 and 7 compare an overtopping event with and without the presence of wind for a mean overtopping discharge of $O(10^2)$ and $O(10^1)$ l/s/m respectively.

In the first case, there were no significant differences comparing wind and no wind conditions (Fig. 6). The wind effect seems to be negligible as compared to the momentum of overtopping water, so that the mean overtopping discharge is not influenced by the wind.

On the other and, for the lower overtopping regime, the overtopping occurs when the wind pushes the droplets behind the structure. Droplets may be indeed carried over the wall under its own momentum without wind, otherwise it falls back into the sea (Fig. 7a). Therefore, for “white overtopping” the onshore wind plays a key role in the overtopping process. The advection of water droplets represents the leading mechanisms in the growth of overtopping rate. Therefore, a depth-integrated numerical model cannot properly reproduce the effect of the wind on the wave overtopping, as observed by Di Leo et al. (2022b).

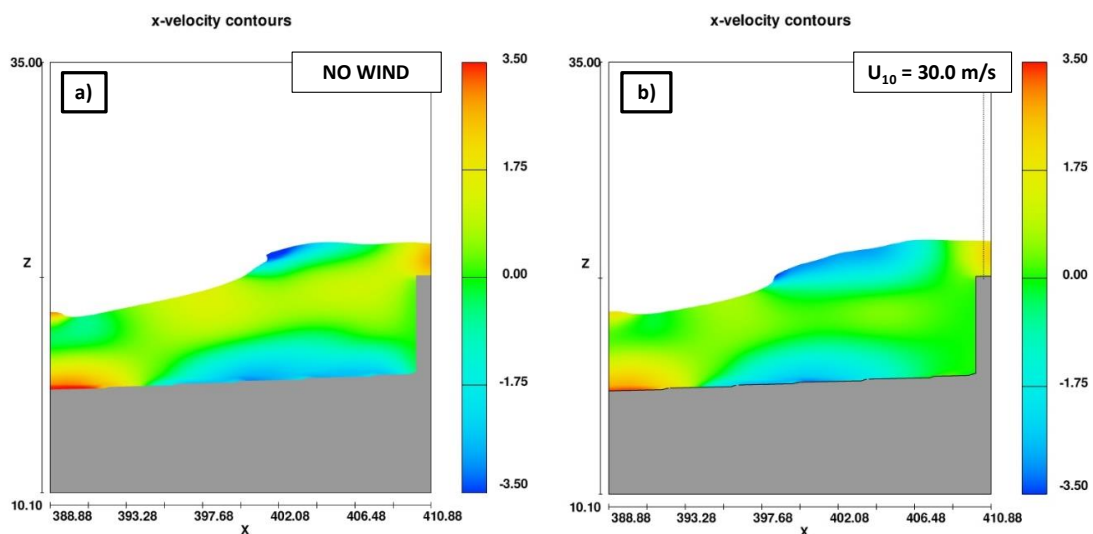


Figure 6. Test with a mean overtopping discharge of the order of 100 l/s/m. Panel a) overtopping event without wind; b) overtopping event with wind.

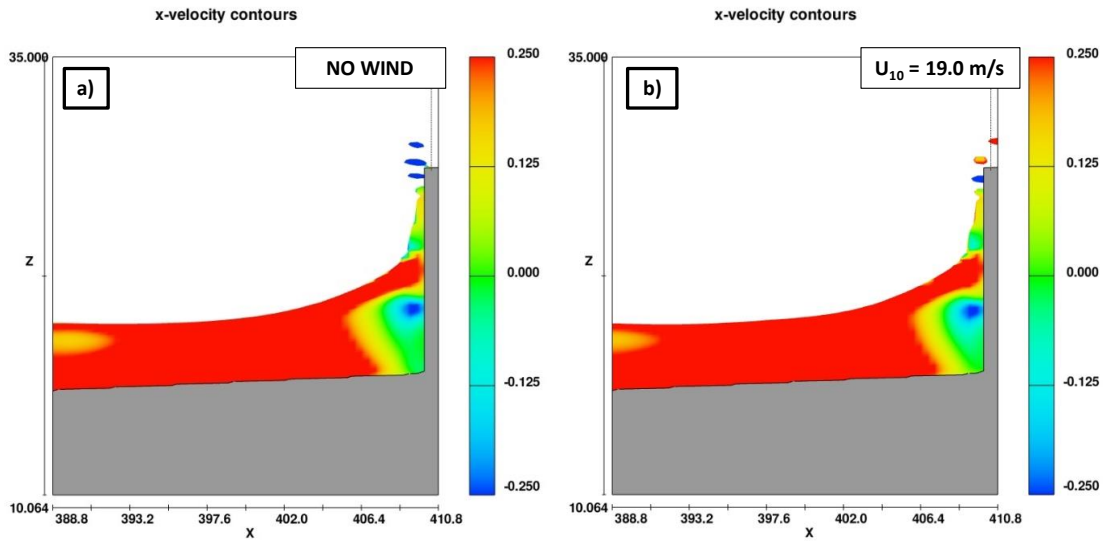


Figure 7. Test with a mean overtopping discharge of the order of 0.1 l/s/m. Panel a) overtopping event without wind; b) overtopping event with wind.

The wind factor f_{WIND}

The wind factor quantitatively indicates the influence of wind on the mean overtopping discharge:

$$f_{WIND} = \frac{q_{WIND}}{q_{NO-WIND}} \quad (9)$$

which, according to Pullen et al. (2009), assumes the following expression:

$$f_{WIND} = 1 + 3 \left(\frac{-\log q_{NO-WIND} - 2}{3} \right)^3 \quad 10^{-5} < q_{NO-WIND} < 10^{-2} \frac{m^3}{sm} \quad (10)$$

Fig. 8a shows numerical wind factors and the Pullen et al.' formula. Both exhibit a decreasing trend with increasing overtopping discharge. However, they differ essentially in two aspects: CFD data provide a maximum value of f_{WIND} of 10 compared to 4 suggested by Pullen et al. 2009; and, according to the Eq. 11, the effect of wind may already be negligible at an overtopping discharge of 1 l/s/m, while the CFD results indicate a strong influence of wind even for larger rates. In Fig. 8b, laboratory data of Durbridge (2021) have been shown as well. Conversely to our experiments, the 2D test carried out at Plymouth University by Durbridge investigate the effect of wave frequency, analyzing regular and irregular waves, while the structure's freeboard and the offshore wave height was left constant. However, numerical and physical results are consistent, showing a significant influence of the wind also for values of $q_{NO-WIND}$ of the order of 10 l/s/m.

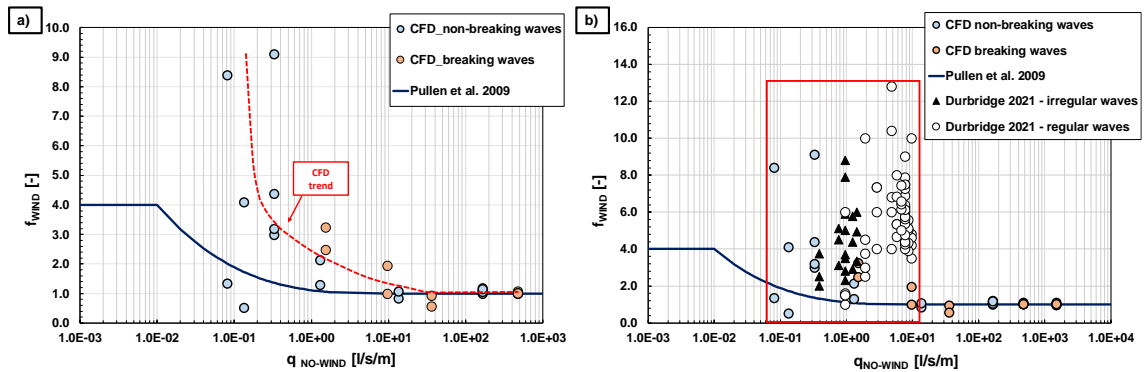


Figure 8. The wind factor as a function of the mean overtopping discharge. Panel a) CFD data vs the formula of Pullen et al. (2009); b) numerical and physical results obtained by Durbridge (2021) compared to the Pullen et al.' formula.

By gathering numerical and Durbridge’s experimental data, we propose a new predictive formula (Fig. 9):

$$f_{WIND} = 1 + 0.00037 \cdot \max\{0.001, q^*\}^{-1.062} S_{s-a} \quad (11)$$

in which q^* is the non-dimensional overtopping discharge:

$$q^* = \frac{q}{\sqrt{gH^3}} \quad (12)$$

and S_{s-a} is the shallow water sea age:

$$S_{s-a} = \frac{U}{\sqrt{gh}} \quad (13)$$

The expression above essentially relates the wind correction factor to the probability of occurrence of water droplets during the overtopping events. The presence of droplets clearly reduces with increasing the relative flow rate q^* (when the overtopping regime tends to “green overtopping”) as well as with increasing water depth. Oppositely, wave breaking occurrence in shallow water increases the generation of droplets, which explains the use of shallow water celerity \sqrt{gh} . Finally, the higher the wind speed the higher the wind factor.

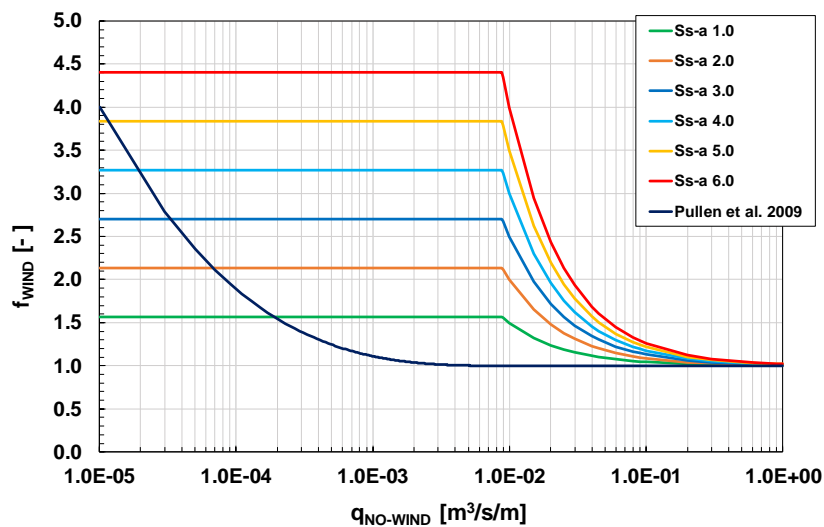


Figure 9. The new wind factor formula proposed by gathering numerical and experimental data compared to those of Pullen et al. (2009).

Fig. 10 shows calculated and measured wind factors, which leads to an R^2 statistics of 0.5. The regression equation resulted however significant at a level of 5%. A low value of R^2 is not surprising since the process which governs the formation of droplets is highly random.

Although the numerical data used to infer Eq. 11 derive from a rough modelling (single-fluid approach), its reliability has been confirmed by comparing computed wind factors with those of Hieu et al. (2014). The latter were obtained by performing numerical experiments with the two-fluids technique. As a further evidence of the ability of the single-fluid approach to correctly reproduce the enhancement of the mean overtopping discharge due to the wind, Fig. 11 indeed shows that results are quite close to the perfect line of agreement.

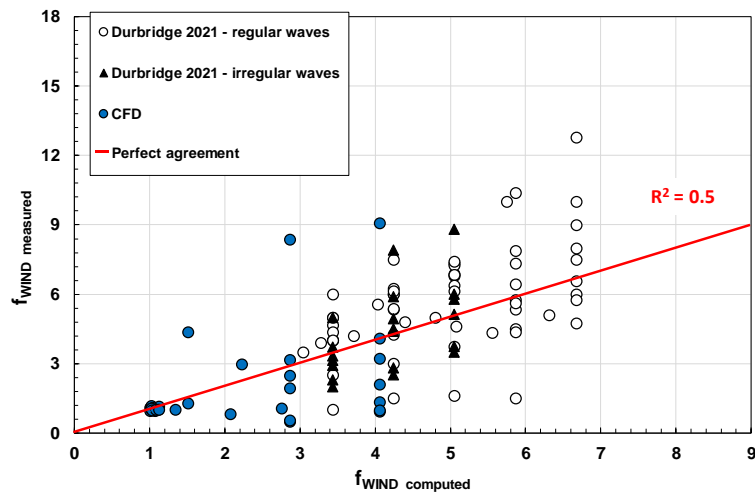


Figure 10. Computed vs measured wind factors.

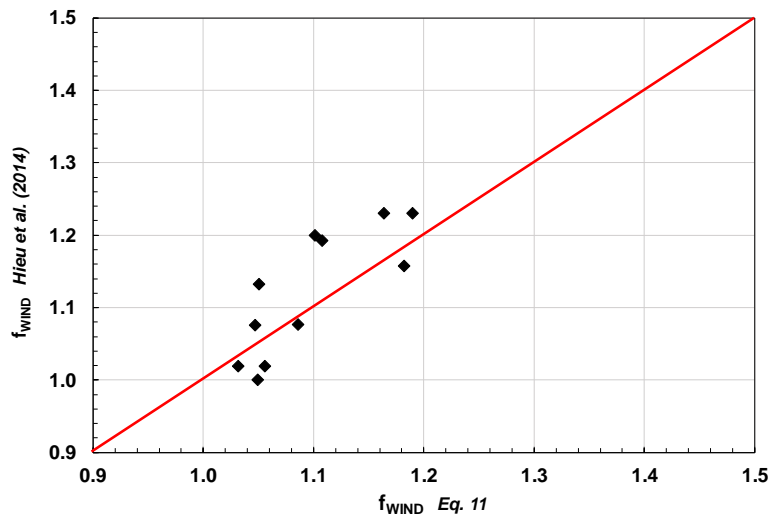


Figure 11. Comparison between wind factors estimated using Eq. 11 and those obtained by Hieu et al. (2014).

CONCLUSIONS

The main purpose of this work was to verify the ability of simplified wind modelling to capture the macroprocesses involved in the phenomenon of wave overtopping in the presence of onshore wind. To this end, a single fluid RANS model has been employed to investigate the wave overtopping of a vertical seawall.

Although the presence of wind has been modelled via the single fluid approach, we demonstrated that an appropriate shear stress can properly reproduce the physical processes observed in the literature. The wind shear stress affects the wave profile by deforming the run-up wedge, moving seaward the breaking point and pushing shoreward the droplets formed in the uprush phase, thus leading to a variation in the overtopping rate. In particular, advection of droplets by the wind behind the seawall plays a key role in enhancing wave overtopping. On the other hand, the variations in the mean water level appear negligible in the numerical experiments performed.

Furthermore, by gathering our numerical results and physical experimental data carried out by Durbridge (2021), a new predictive equation was proposed to quantify the effect of the wind on the mean overtopping discharge. The new formula relates the wind factor to the mean overtopping discharge, the wind speed and the water depth.

Future research will adopt the two-fluids approach to analyze the influence of wind on wave overtopping. The aim is twofold: to further understand the process and to evaluate the impacts of the wind modelling used on the results.

REFERENCES

- Andreas, E.L., L. Mahrt, D. Vickers. 2012. A New Drag Relation for Aerodynamically Rough Flow over the Ocean, *Journal of the Atmospheric Sciences*, 2520–2537.
- Bretschneider, CL. 1964. Generation of waves by wind: state of art. *Presented at International Summer Course*, Lunteren, Netherlands. September 1- 18.
- Buccino, M., M. Daliri, F. Dentale, A. Di Leo, M. Calabrese. 2019a. CFD experiments on a low crested sloping top caisson breakwater. Part 1. nature of loadings and global stability, *Ocean Engineering*, 182, 259–282.
- Buccino, M., M. Daliri, F. Dentale, M. Calabrese, 2019b. CFD experiments on a low crested sloping top caisson breakwater. Part 2. Analysis of plume impact. *Ocean Engineering*, 173, 345–357.
- Dentale, F., F. Reale, A. Di Leo, E. Pugliese Carratelli. 2018. A CFD approach to rubble mound breakwater design. *International Journal of Naval Architecture and Ocean Engineering*, 10(5), pp. 644–650.
- de Waal, J.P., P. Tönjes, J. van der Meer. 1996. Wave overtopping of vertical structures including wind effect, *Proceedings of the 25th International Conference on Coastal Engineering*, ASCE, Orlando, FL, USA, 2–6 September 1996.
- Di Leo, A., M. Buccino, F. Dentale, E. Pugliese Carratelli. 2022a. CFD Analysis of Wind Effect on Wave Overtopping, *Proceedings of the 32nd International Ocean and Polar Engineering Conference*, Shanghai, China, 5–10 June 2022.
- Di Leo, A., F. Dentale, M. Buccino, S. Tuozzo, E. Pugliese Carratelli. 2022b. Numerical Analysis of Wind Effect on Wave Overtopping on a Vertical Seawall, *Water*, 14, 3891.
- Durbridge, S. 2021. The effect of onshore wind on wave overtopping of a vertical sea wall. *Plymouth Stud. Sci.*, 14, 311–355.
- Fenton, J.D. Numerical Methods for Nonlinear Waves, *Advances in Coastal and Ocean Engineering*, Liu, P.L.-F., Ed.; World Scientific: Singapore, 1999; Volume 5, pp. 241–324.
- Flow Science, Inc. *FLOW-3D User's Manual*, HYDRO ed.; Flow Science, Inc.: Santa Fe, NM, USA, 2022.
- Hieu, P.D., P.N. Vinh, D.V. Toan, N.T. Son. 2014. Study of Wave-wind Interaction at a Seawall Using a Numerical Wave Channel, *Applied Mathematical Modelling*, 38, 5149–5159.
- Hirt, C.W., and B.D. Nichols. 1981. Volume of fluid (VOF) method for the dynamics of free boundaries, *Journal of Computational Physics*, 39, 201–225.
- Hirt, C.W., and J.M. Sicilian. 1985. A porosity technique for the definition of obstacles in rectangular cell meshes, *Proceedings of the Fourth International Conference of Ship Hydrodynamics, National Academy of Science*, Washington, DC, USA, 24–27 September 1985.
- Kiku, M., and K. Kawasaki. 2014. Proposal of numerical wave flume for wave overtopping computation considering wind external force, *Proceedings of 34th Conference on Coastal Engineering*, Seoul, Republic of Korea, 15–20 June 2014.
- Lopez, L.F.C., D. Salerno, F. Dentale, A. Capobianco, M. Buccino. 2015. Experimental campaign on the overtopping of the seawall Malecon Traditional, *Proceeding of 25th International Ocean and Polar Engineering Conference, ISOPE Kona*, Big Is-land, United States, 21-26 June 2015, pp. 1499-1505. Volume 2015-January
- Lopez, L. F. C., D. Salerno, F. Dentale, A. Capobianco, Buccino, M. 2016. Wave overtopping at Malecòn tradicional, La Habana, Cuba. *Coastal Engineering Proceedings*, Antalya, Turkey, 17-20 November 2016, pp.24-24.
- Murakami, K., D. Maki, K. Ogino. 2019. Effect of Wind Velocity on Wave Overtopping, *Proceedings of the 10th International Conference on Asian and Pacific Coasts (APAC 2019)*, Hanoi, Vietnam: 25 – 28 September.
- Perlin, M., C. Wooyoung, T. Zhigang, 2013. Breaking Waves in Deep and Intermediate Waters. *Annual Review of Fluid Mechanics*, 45, 115–145.
- Pullen, T., W. Allsop, T. Bruce, J. Pearson. 2009. Field and laboratory measurements of mean overtopping discharges and spatial distributions at vertical seawalls, *Coastal Engineering*.
- Resio, D.T. 1987. Assessment of Wind Effects on Wave Overtopping of Proposed Virginia Beach Seawall. *Tech. Memo to CERC.*, OCTI.
- Xie, Z. 2014. Numerical modelling of wind effects on breaking solitary waves, *European Journal of Mechanics - B/Fluids*, 43, 135–147.
- Yakhot, V., L.M. Smith. 1992. The renormalization group, the ϵ -expansion and derivation of turbulence models, *Journal of Scientific Computing*, 7, 35.